Performance Investigation and Adaptive Neuro-Fuzzy Prediction of Building Integrated Straight-Bladed Vertical Axis Wind Turbine

*Mohammed Gwani
Department of Physics, Kebbi State University of Science and Technology, Aliero, Nigeria
Corresponding Author's email: gwanimohammed@gmail.com

Abstract

This paper presents the performance investigation and adaptive neuro-fuzzy prediction of a building integrated straight-bladed vertical axis wind turbine (VAWT). An experiment was conducted with the VAWT integrated on the building rooftop. The coefficient of power of the VAWT was predicted using adaptive neuro-fuzzy inference system (ANFIS). The input variables for the model development include the rotational speed, angular velocity, and tip speed ratio, while coefficient of power is the output. In the fuzzy logic of the fuzzy inference system (FIS), the parameter of the membership function is adjusted by the neural network in ANFIS. MATLAB/Simulink was used to implement this intelligent algorithm and the performance was investigated using root mean square error (RMSE) and coefficient of determinant (R^2). In addition, the ANFIS technique precision was evaluated against the results of the experiment. The result obtained indicates that the maximum coefficient of power (C_{pmax}) was obtained at about $Y = 250$ mm above the building rooftop. Furthermore, it was also established that the developed ANFIS model is very effective and reliable in predicting the performance of building integrated straight-bladed VAWT.

Keywords: Coefficient of power; Wind turbine; Adaptive neuro-fuzzy; ANFIS; Power, Torque

1. Introduction

Globally, progresses in wind energy research continue to be strong with more active countries and players [1]. Being a clean source of renewable energy, wind energy has been gaining more attention recently and is fast growing all over the world with increasing trend in worldwide installed wind power capacity since the beginning of the 21st century [2]. The global installed wind capacity at the end of 2016 was around 486 GW, up from 17 GW at the end of 2000. In 2016 alone, 54 GW of new wind capacity were added [3]. The development of small wind turbine has rekindled the hope and the possibility of harnessing wind power for on-site energy generation or domestic production. Building rooftop can be an excellent location for wind turbines, both for on-site energy generation, or to take advantage of the faster wind at the rooftop while reducing the cost of support towers [4].

Wind turbine can be integrated into the urban buildings as building integrated/roof mounted wind turbines [5-10], or building augmented wind turbine [11-15]. Majority of the actual installation of wind turbine in the urban environment is the horizontal axis wind turbine (HAWT) [13]. Ordinarily, HAWT are design for an open site, therefore, mounting HAWT in the urban environment is tantamount to many different challenges

like complex wind conditions of the urban environment, the use of yaw mechanism and the dangers it poses to the surroundings. In view of these, many recent studies on the mounting of wind turbine in the urban environment focus on the vertical axis wind turbine (VAWT). The VAWT is omni-directional, has easier installation processes, operations and maintenance when compared to the HAWT. However, the set-backs of this type of wind turbine are that it cannot self-start at low wind speed [16-20]. To overcome these challenges, many researchers have proposed the idea of integrating the VAWT systems onto the urban buildings to gain benefit of the increase wind speed at the building rooftop [21-29]. These systems features either additional augmentation system [21-23], or retrofitting onto the building by utilizing the building geometry [24-29].

In this study a straight-bladed VAWT has been integrated onto a building model with vaulted rooftop and tested in an experiment. The data obtained from this study were used as input parameters to further predict the power coefficient of the building integrated straight-bladed VAWT using the soft computing methodology. The key goal was to develop an ANFIS model that can predict the wind turbine power coefficient. Even though, a quite number of models have been proposed for estimating the performance of wind turbine, however there are some

limitations associated with these models, which include computational time and accuracy. To overcome these challenges, a substitute to analytical approach which is artificial neural networks (ANN) can be used. ANN offers favorable circumstance and provides minimal answers to multivariable issues [30-34]. As hybrid method, ANFIS has the ability to learn and adopt automatically; it has good learning and prediction capabilities, and it is an efficient tool to deal with when encountering doubts in any system [35]. The fuzzy inference systems are merged with a neural network learning algorithm by the ANFIS to estimate the performance of building integrated wind turbine using a soft computing technique. The proposed system was obtained from the gathered input/output data sets, and through a complete investigation of the data for the ANFIS system was train and checked.

Many studies have been reported for the performance prediction of wind turbines in the urban environment. Petkovic et al. [36] estimated building power augmentation using a simple turbine model using an ANFIS methodology. The result obtained demonstrated that the developed method is very effective. The application of ANFIS for the investigation of power augmented VAWT performance has been reported by Chong et al. [37]. The results obtained demonstrated that the developed method is very effective. Shamshirband et al. [38] uses the ANFIS methodology to predict the wake added turbulence in a wind turbine, the results obtained show the effectiveness of the developed method. Other studies that uses soft computing methodology to predicts the performance of wind turbine are reported in [39, 40].

1.2 Wind turbine power
Estimating how much energy will be produced by a wind turbine is a very important step in designing a wind turbine. This means that accurate calculations of the energy are very important to strike a balance between the cost and energy produced as well as to forecast for the expected energy to be generated at a particular location. The wind turbine power can be calculated using Equation 1.

$$P = C_p \rho A U_\infty^3 \qquad (1)$$

Where P = available power in the wind, (W), ρ = density (kg/m^3), u_∞ = wind speed (m/s), A = swept area of the turbine (m^2).

The efficiency with which energy is transferred from wind to the wind turbine rotor often determines the actual power produced by a wind turbine. This is called the coefficient of power (C_p) which is the ratio of the actual power developed by the wind turbine to the theoretical power available in the wind. It can be calculated from Equation 2 as

$$C_p = \frac{p}{0.5\rho A U_\infty^3} \qquad (2)$$

where C_p is the power coefficient of the wind turbine.

The Coefficient of the torque (C_T) is the ratio between the actual torques developed by the rotor to the theoretical torque and it is given by

$$C_T = \frac{2T}{\rho A U_\infty^3 R} \qquad (3)$$

Where T is the actual torque developed by the rotor; R is the radius of the turbine (m).

The C_p and the C_T depends on the tip speed ratio (TSR), (λ) of the wind turbine blade which is the ratio of the wind speed at the tip of the blade to the free stream wind velocity. Wind turbines are designed to operate at their optimum TSR in order to obtain maximum and optimal rotor efficiency. The TSR depends on a particular wind turbine design, the airfoil profile, and the number of blades used [41]. The TSR is given by

$$\text{Tip speed ratio: } \lambda = \frac{\omega R}{u_\infty} = \frac{2\pi N R}{u_\infty} \qquad (4)$$

Where ω is the angular velocity (rad/s) and N is rotational speed of the rotor.

2. Materials and Method
2.1 Design Description of The Vertical Axis Wind Turbine (VAWT)
VAWT used for this study is a straight-bladed turbine, which functions with airflows coming from any horizontal directions. It comprises three vertical blades and six supporting struts made of flat metal plates with width and thickness of 25 mm and 2.03 mm respectively. The supporting struts connect the vertical blades to the drive shaft which in turn is connected to the generator. The general arrangement and the top view of the turbine are shown in Figures 2.1 (a) and 2.1(b), while the lab scale model for this turbine is presented in Figure 2.2. The vertical blades are connected to the center shaft via supporting struts. The lower and upper parts of the supporting struts are placed at a relative distance of 100 mm. The profile of the airfoil used for the straight-bladed VAWT is a symmetrical airfoil, NACA 0015 airfoil. The advantage of using NACA 0015 is that this set of airfoil have a well-documented lift, drag and pitching moment characteristics thus making validation of theoretical predictions easier [42, 43]. The specification of the turbine is given in Table 2.1.

Table 2.1: Dimensions of the VAWT

Parameters	Units	Material
Diameter of rotor, d	35 cm	-
Span length of vertical blade l	30 cm	-
Chord length of vertical blade, c	5 cm	-
Wind speed U_∞	4.5 m/s	-
Type of aerofoil	-	Symmetrical aerofoil
Profile of aerofoil	NACA 0015	-
Pitch angle of the vertical blade, β	0º	
Supporting struts	Width = 25 mm, thickness = 2.03 mm	-
Generator	10 W	
Shaft	-	Mild steel
Vertical blade	-	Carbon fibre
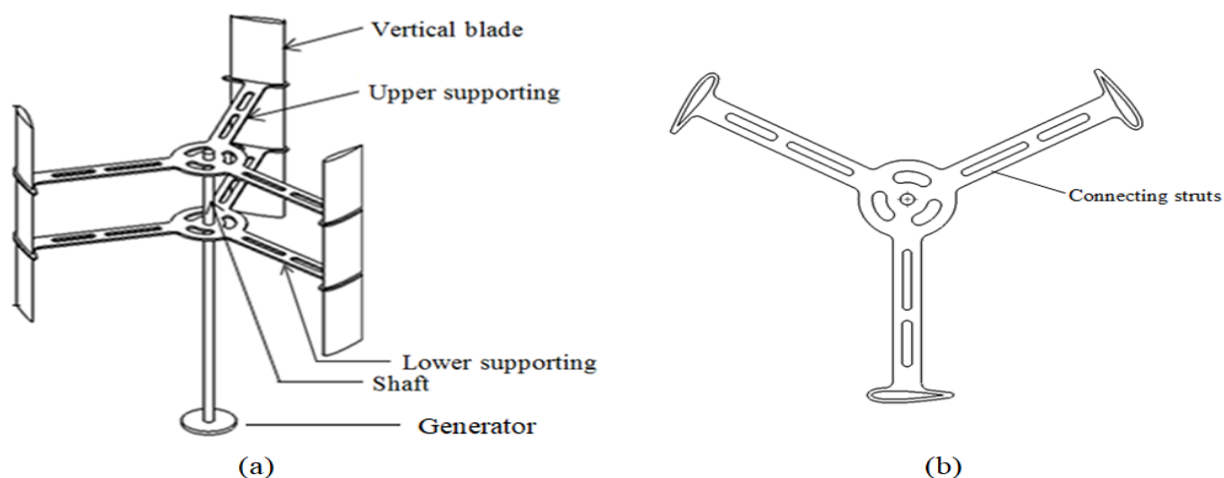
Figure 2.1: (a) General Arrangement of VAWT, (b) Top View of the VAWT

Figure 2.2: Lab Scale Model for the VAWT

2.2 Experimental Set-up and Procedures

A building model with vaulted roof shape was fabricated for the integration of a VAWT at the rooftop. The height, length, and width of building model are 1364 mm x 1450 mm x 740 mm respectively. The experimental set-up for the building integrated VAWT is shown in Figure 2.3 and the schematic diagram of the building model with the VAWT mounted at the rooftop and the dimension of the ventilation fans is shown in Figure 2.4. An average wind speed of 4.5 m/s ± 0.2 m/s is used for this experiment. The wind source was generated from a ventilation fans which are arranged in an equally spaced 3 x 3 grid points. The wind speed measurements were taken downstream of the ventilation fans using a Vane-type anemometer as shown in the experimental set-up in Figure 2.3. The rotor of the VAWT was in free-running conditions. Using a controller system, the performance of the building integrated VAWT were logged. The recorded parameters for the study include rotational speed (RPM), voltage, and the current; with these values of the current and voltage the electrical power generated by the wind turbine is calculated, using the dynamometer controller system the alternating current voltage from the generator

is rectified to direct current. The measurement of the rotor rotational speed was conducted during free-running conditions where the rotor is subjected to inertia and bearing friction with no external loads applied during this assessment. The rotational speed was measured continuously in seconds interval until the stabilized rotational speed of the rotor is achieved.
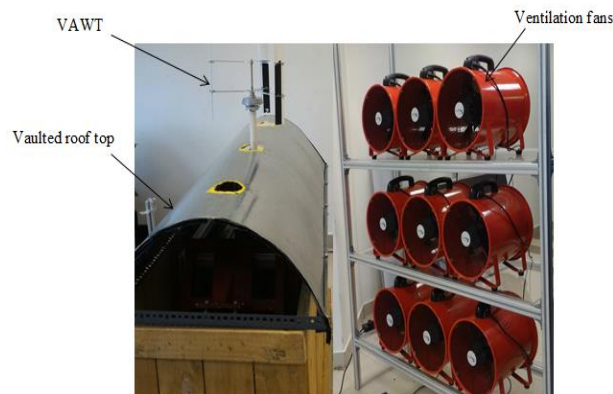

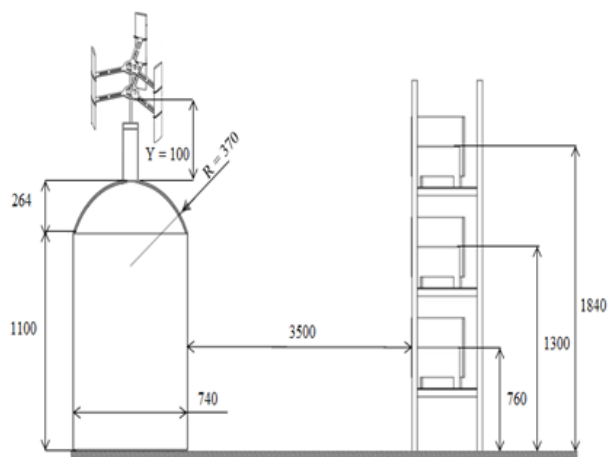**Figure 2.3:** Experimental set-tup for the VAWT

Figure 2.4: Schematic Diragram of Building Model With Dimensions (All Dimension are in mm)

2.3 ANFIS Input Parameters

The ANFIS is a data-driven model which depends on the input parameters selections to make reasonable predictions. In view of these, it is very important to adequately consider the factors that control the system studied in order to develop a network that is reliable [44]. Therefore, the rotational speed (RPM), angular velocity (ω), and tip speed ratio (λ) extracted from the experimental study of the building integrated VAWT were use as the inputs for the learning techniques. The experimental data were acquired for various VAWT heights from $Y = 100$ mm- 250 mm at the rooftop. 70% of the data from the experiment were used to train samples while the samples were tested using the remaining 30%.

2.4 Adaptive Neuro-Fuzzy Application

ANFIS is an exceptional neural network with an excellent learning and forecasting skills [45]. Due to the outstanding skills of the ANFIS technique several engineering systems previously used this technique in the performance predictions of various engineering systems [46-48]. Owing to these capabilities, ANFIS technique is very reliable in dealing with encountered doubts in any system [49-51]. The Fuzzy logic (FL) has 2 significant benefits in the analysis of data as compared to conventional methods. One of these benefits is the incorporation within its mapping rules the qualitative aspect of human experience, which provide a way for catching information. The second benefit is the reduction of possible difficulties in the modelling and analysis of complex data. Furthermore the models of complex systems were also identified by Artificial neural networks (ANNs) [52]. To simplify a complex task, ANNs and FL are combined together for the same purpose to take the advantage of the modelling superiority of FL and the learning capability of ANNs. This is referred to as ANFIS. Since ANFIS learns from training data set, therefore with an appropriate training structure and sufficient clean data-set, ANFIS can correctly estimate the performance of building integrated VAWT [11].

The main core of ANFIS is the Fuzzy Inference System (FIS). The FIS can be used to forecast the behavior of numerous systems that are ambiguous this is because it is established on expertise which is expressed in 'IF-THEN' rules. No knowledge of fundamental physical process is needed for the precondition of the applications of the FIS; this is seen as one of the advantages of the FIS. In view of these, the FIS is incorporated by the ANFIS through the neural network back-propagation learning algorithm, therefore enabling the fuzzy logic to acquaint with the membership function parameters by allowing the related FIS to track the input and output data [53-55].

The FIS basic structure consists of three (3) components; the rule base, the database and the reasoning mechanism. The fuzzy rules are selected by a rule base, and the membership functions (MFs) used in the fuzzy rules is explained by database. The reasoning mechanism uses the inference procedure to derive genuine output and deductions. The knowledge and technique from different sources including their methodologies were combined with these intelligent systems. Within a specific domain, they possess human-like expertise that learns to familiarize them to do better in varying environments. The ANFIS based on input-output data collection was tuned by using the Back-propagation algorithm.

In this study, the coefficient of power (C_p) of a building integrated VAWT was estimated using an established ANFIS model. For any given number of data inputs, the

optimal parameters were determined by the ANFIS networks. MATLAB Fuzzy logic toolbox was use for the whole training and assessment process of the fuzzy inference system. Since there one output to determine, three ANFIS networks were modeled. The ANFIS structure with three inputs, L, M and N is shown in Figure 2.5.
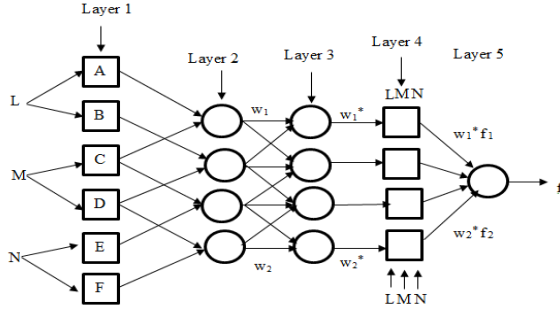

Figure 2.5: ANFIS Structure

In this study, the first-order Sugeno model is used. The model has two inputs and fuzzy "IF-THEN" rules of Takagi and Sugeno's types;

$$if\ L\ is\ A\ and\ M\ is\ C\ and\ N\ is\ E\ then\ f_1 = p_1L + q_1M + r_1N + t \tag{5}$$

The first layer comprises of the input variable membership functions (MFs); it has two inputs (1 & 2) values which were delivered to the subsequent layer. Every node in this layer is an adaptive node and has a node function.

$$O = \mu(L, M, N)_i \tag{6}$$
where $\mu(L, M, N)_i$ are MFs

For this study, the bell-shaped MFs with maximum equal to 1 and minimum equal to 0 is selected.

$$f(L; a, b, c) = \frac{1}{1+\left(\frac{L-c}{a}\right)^{2b}} \tag{7}$$

The three parameters, x, y, and z determined bell-shaped function where y is positive and z is located at the center of the curve as shown in Figure 2.6.
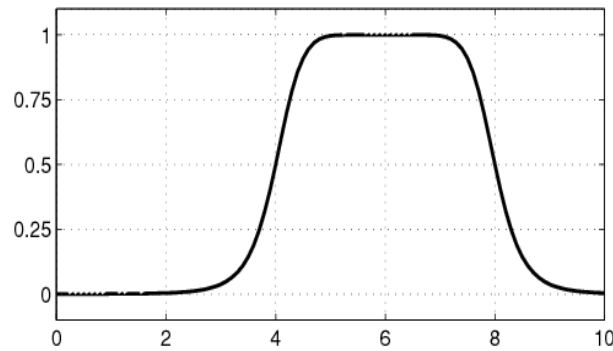

Figure 2.6: Bell-Shaped Membership Function (x=2, y=4, z=6)

The second layer (i.e. membership layer) accepts the input values from the first layer. The weight of each MFs is checked on this second layer and individual input variable is represented by MFs which acts as fuzzy sets. In this layer every node is non-adaptive, and the incoming signals is multiplied by this layer and sends the product out as shown in the Equation 8 below:

$$w_i = \mu(L)_i * \mu(L)_{i+1} \tag{8}$$

Each node output represent the firing strenght of a rule or weight.

The rule layer is the third layer. In this layer each node (each neuron) does the pre-condition matching of the fuzzy rules; the level of activation of each rule is calculated with equal number of layers and fuzzy rules. Furthermore, as a non-adaptive layer, each node calculates the weights which are normalized, and the ratio of the rule's firing strength to the sum of all the rules' firing strength as shown in Equation 9 below:

$$w_i^* = \frac{w_i}{w_1 + w_2}\ \ for\ i = 1, 2 \tag{9}$$

This layer's outputs are called normalized weights or normalized firing strenghts.

The output values which results from the inference of the rules were provided by the fourth layer which is known as the normalised firing strengths or normalised weight. It is also known as the defuzzification layer. In this layer, each node is an adaptive node with a node function.

$$O_i^4 = w_i^* Lf = w_i^*(p_iL + q_iM + r_i) \tag{10}$$

In this layer, p_i, q_i, r_i is the consequent parameters.

The fifth layer summed up all the incoming inputs from the fourth layer and the classification results from the fuzzy are transformed into a crisp (binary) output. The overall output are computed in the fifth layer by the single non-adaptive node.

$$O_i^5 = \sum_i w_i^* Lf = \frac{\sum_i w_i f}{\sum_i w_i} \tag{11}$$

The hybrid learning algorithms were used to identify the parameters in the ANFIS architecture. Functional signals go frontward up to Layer 4 in the forward pass of the hybrid learning algorithm and the least square estimate is used to identified the consequent parameters. The gradient descent updates the premise parameters in the backward pass while the error rates propagate backwards.

3. Results and Discussion

For this work, initial experiments were conducted with the VAWT integrated on the building rooftop while the turbine was placed at a varying height of $Y = 100$ mm - 250 mm above the building rooftop. The parameters measured from the experiments include the RPM, the

current and voltage while the angular velocity ω, and tip speed ratio TSR were calculated using their appropriate equations. Then the data obtained from the experiment were used as the input parameters for the ANFIS prediction model of the building integrated VAWT.

3.1 Experimental Results

Figure 3.1 presents the C_p values against TSR (λ) for the building integrated straight-bladed VAWT mounted at varying height of $Y = 100$ mm - 250 mm on a building rooftop.
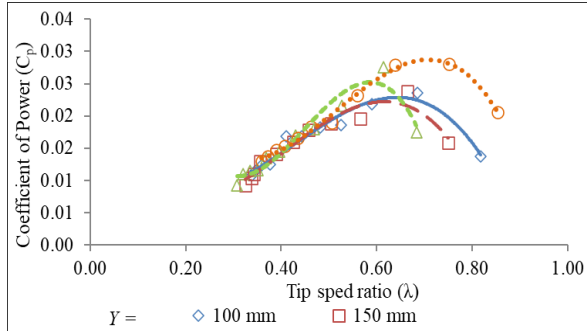

Figure 3.1: Coefficient of Power against Tip Speed Ratio (y =100 mm – 250 mm)

From this Figure, the trend shows that the C_p values increases with TSR and then attain its peak value at certain value of TSR (λ) before decreasing with increase in λ. In addition, the C_p values increases with increase in the height of turbine above the rooftop. However, VAWT mounting at closer height to the rooftop has lower C_p values compared to the one mounted at higher heights. The maximum C_p value obtained at the height of y = 100 mm was 0.0235 at TSR 0.68. As the height increased above the rooftop to 250 mm, the maximum C_p values increases from 0.0235 at TSR 0.68 to 0.0281 at TSR 0.75, indicating an increment of 20% in the C_p value at $Y = 250$ mm. The poor performance of the turbine at lower height above the rooftop was due to the high level of turbulence experienced by the turbine at lower height ($Y = 100$ mm). However, its performance may increase due to the fact that the turbine can operates at a low turbulence zone as it moves further away from the building rooftop. The summary of the results is presented in the Table 3.1.

Furthermore, Figures 3.2 and 3.3 illustrates the rotational speed against time, and the power against TSR by the building integrated VAWT for y =100mm - 250 mm. As depicted in the Figure 3.2, the trends of the rotational speed for the wind turbines are steadily increasing with time and then stabilised after reaching a steady-state. Although, the results showed that the maximum rotational speed of the turbine increase steadily with height, the rotational speed obtained at $Y = 250$ mm is higher compared to RPM of the turbine at $Y = 100$ mm closer to the rooftop. Thus, this indicates that, the turbine has a better rotational speed when mounted at higher

height above the rooftop due to less turbulence experience at that position.

For the power produced (Figure 3.3), the graph shows similar trend where the power increases with TSR and the peak power obtained for the entire configuration was 0.073 W at a TSR of 0.75 and at a height of $Y = 250$ mm.
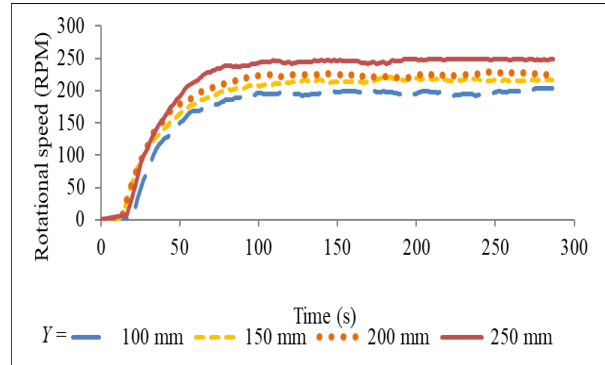

Figure 3.2: Rotational Speed against Time (for $Y = 100m$ - 250 mm)
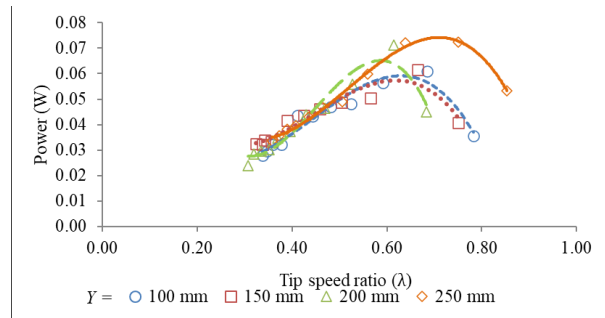

Figure 3.3: Power Produced against Time (for $Y = 100m$ - 250 mm)

In Addition, Figure 3.4 present the peak power produce by the building integrated VAWT at various height above the rooftop. It can be seen form this Figure that, at Y = 100 mm, the peak power produced by the turbine was 0.06 W, however, when the height was increased to Y = 250 mm, the peak power increases to 0.073 W. This demonstrate that the power produced by the building integrated VAWT increases with increase in height. The reason for the improve performance of the building integrated VAWT at higher height is due to the increase wind speed experienced by the wind turbine at higher height.
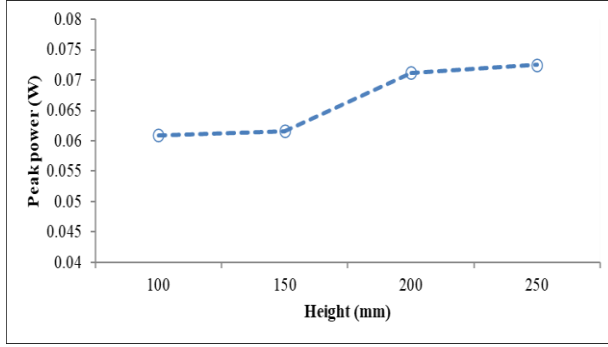
Figure 3.4: Peak Power at Different Heights

Figure 3.5 presents the coefficient of torque against the TSR. From this Figure, the data indicates that the torque coefficient produced by the VAWTs significantly increased with increase in height above the roof top. However, the torque coefficient C_T decreases with increase in λ. The low coefficient of torque values generated by the turbine at lower heights is attributed to the supporting struts which produce additional parasitic drag that affect the overall output of the building integrated VAWT. At Y = 250 mm height peak coefficient of torque produced by the VAWT is 0.048 at TSR of 0.64, which is 9.1% higher than at Y = 100 mm.
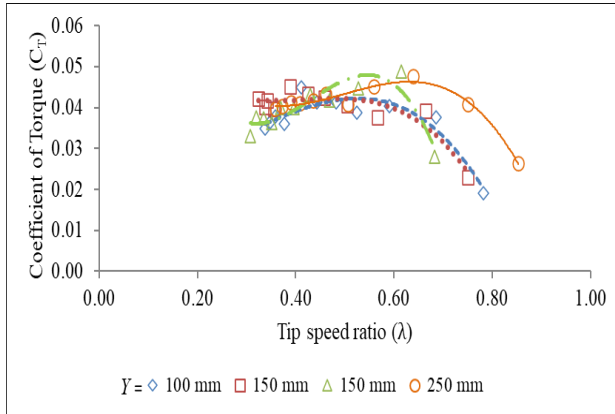

Figure 3.5: Coefficient of Torque against TSR (λ) (for Y= 100 mm – 250 mm)

Table 3.1: Summary of Experimental Results on Variation of Height

Parameter	Height (mm)			
	100	150	200	250
RPM	204	221	229	249
C_{Pmax}	0.0235	0.0238	0.0276	0.0281
TSR for C_{pmax}	0.68	0.66	0.61	0.75
C_T	0.044	0.045	0.048	0.048
Power	0.061	0.062	0.071	0.073

3.2 ANFIS Estimation for the Performance of Building Integrated Straight-Bladed VAWT

The ANFIS model for the performance prediction of the coefficient of power of the building integrated VAWT was evaluated using the following statistical indicators; Root Mean Square error (RMSE), coefficient of determination (R^2), and the correlation coefficient (r) defined by Equations (12-14) in the assessment of the models' predictive performance and accuracy.

$$RMSE = \sqrt{\frac{\sum_{i=1}^{n}(P_i - O_i)^2}{n}} \tag{12}$$

$$R^2 = \frac{[\sum_{i=1}^{n}(O_i - \bar{O}_i)(P_i - \bar{P}_i)]^2}{\sum_{i=1}^{n}(O_i - \bar{O}_i)\sum_{i=1}^{n}(P_i - \bar{P}_i)} \tag{13}$$

$$r = \frac{n(\sum_{i-1}^{n} O_i \cdot P_i) - (\sum_{i-1}^{n} O_i) \cdot (\sum_{i-1}^{n} P_i)}{\sqrt{(n\sum_{i-1}^{n} O_i^2 - (\sum_{i-1}^{n} O_i))^2 \cdot (n\sum_{i-1}^{n} P_i^2 - (\sum_{i-1}^{n} P_i))^2}} \tag{14}$$

Where P_i and O_i are the experimental and forecast values, respectively and *n* is the total number of test data. The experimental data obtained from the experiments was used for the training of the ANFIS network. During the training procedure three bell-shaped MFs were used for input fuzzyfication. The statistical indicators (RMSE and R^2) have been used to assess the performance prediction of the ANFIS models (Table 3.2) while Figure 3.6 gives the scattered plot for the ANFIS prediction and actual values of the coefficient of power (C_p) of the VAWT integrated on the building.

Table 3.2: ANFIS prediction errors

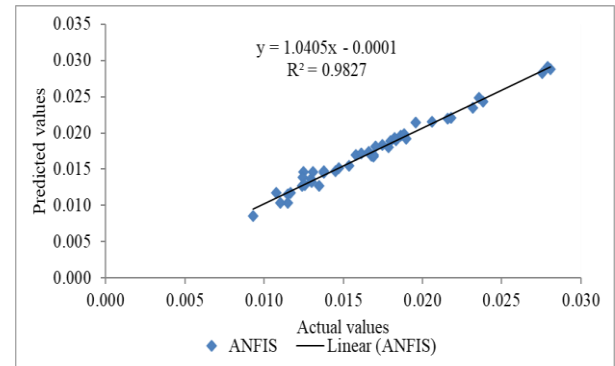| Time step	RMSE	R	R^2
C_P	0.00088	0.99133	0.9827

Figure 3.6: Scattered Plot of Predicted and Experimental Data for Coefficient of Power

From this Figure, the linear relationship of the model with real data illustrates the capability of the ANFIS model in predicting the coefficient of power of the building integrated VAWT. Also, from this Figure, the R^2 value is high indicating a good correlation between the predicted values by the ANFIS model and the actual

values from the experimental data. With this output from the ANFIS model, one can conclude that this model can be used to predict the C_p values of the building integrated VAWT. By feeding the ANFIS model with the rotational speed, angular velocity and tip speed ratio, the coefficient of power output of the building integrated VAWT can be predicted. The predicted output data from the ANFIS can be used as an effective indicator to assess the performance of the building integrated VAWT.

The assessment of the ANFIS model performance for the prediction of the C_p values was conducted in a palpable manner base on the RMSE and R^2. The results presented in Table 3.2 shows the RMSE, r, and R^2 values for the parameter considered for this study. The results indicate that the ANFIS model proposed can be used for predicting the C_P values of the building integrated VAWT with high accuracy and reliability. The accuracy and reliability of ANFIS in predicating the performance of wind turbine was reported in [11, 39].

Based on the output which was obtained from the ANFIS model, it can be concluded that the model can be used to forecast wind turbine performance for any future building in the urban environment. By feeding the experimental data such as RPM, ω, and TSR (λ) of the building integrated wind turbine into the ANFIS model, the output i.e. coefficient of power of the building integrated wind turbine can be predicted with a reduce cost and time. For the current study, the following experimental data; RPM, ω, and TSR (λ) were used to train the ANFIS model. For future study, larger range data from a large scale building integrated wind turbine can be used to train and test the ANFIS model.

4. Conclusion

In this work, building integrated wind turbine was suggested as an effective solution for on-site energy generation for buildings with the sole aim of promoting zero energy buildings. VAWT is considered to be more suitable to be integrated onto the urban building because of the advantages it has over the HAWT. In this study, a building integrated VAWT was design and tested experimentally and the coefficient of power of the building integrated VAWT was predicted by the application of ANFIS methodology, the accuracy of the ANFIS method in predicting the performance of building integrated VAWT was tested. The ANFIS technique investigated how accurate the coefficient of power of the building integrated straight-bladed VAWT can be estimated. As parameters for the measurement of the performance of wind turbine, the RPM, ω, and TSR (λ) were used as the input parameters in the developed ANFIS model. ANFIS was chosen because it is well-adaptable with optimization and adaptive techniques as well as computationally efficient. The result obtained from the experimental study was compared against the ANFIS predicted results. The findings showed that the

ANFIS technique can accurately predict the performance of building integrated straight-bladed VAWT with high precision and reliability.

References

1. International Energy Agency IEA. Technology Road Map Wind Energy. Paris Cedex 15, France: 2013.
2. REN 21. Renewable Energy Policy Network for 21 Century. 2014.
3. Ren 21. Renewable energy policy network for the 21st century. Retrieved from Robert, H., Ning, Q., Jonathan, E., Naveed, D. I. Wind tunnel and numerical study of a small vertical axis wind turbine. Renewable Energy. 2014 a(5):412-22.
4. Casini M. Small Vertical Axis Wind Turbines for Energy Efficiency of Buildings. Journal of Clean Energy Technologies. 2016; 4(1).
5. Abohela I, Hamza N, Dudek, S. Urban Wind Turbines Integration in the Built Form and Environment. Forum e-journal 10 Newcastle University. 2011; 23-39.
6. Beller C. Energy Output Estimation for a Small Wind Turbine Positioned on a Rooftop in the Urban Environment with and without a Duct. National Laborator for Sustainable Energy. 2011; 0106-2840 ISSN 978-87-550-3721-2.
7. Perwita Sari D, editor Measurement of the Influence of Roof Pitch to Increasing Wind Power Density. Conference and Exhibition Indonesia - New, Renewable Energy and Energy Concervation, [The 3 rd Indo EBTKE ConEx 2014]; 2015 Indonesia.
8. Muller G, Jentsch M, Stoddart E. Vertical axis Resistance Type Wind Turbines for use in Buildings. Renewable Energy. 2009; 34:1407-12.
9. Dutton AG, Halliday JA, Halliday MJ. The Feasibility of Building Mounted/Integrated Wind Turbines (BUWTs): Achieving their Potential for Carbon Emission Reductions. Energy research Unit, Rutherford Appleton Laboratory, Science and Technology Facilities Council. Final Report of Carbon Trust Contract: 2002-07-028-1-6, Oxfordshire, United Kingdom, 2005.
10. Walker SL. Building Mounted Wind Turbines And Their Suitability for the Urban Scale- A Review of Methods of Estimating Urban Wind Resource. Energy and Buildings. 2011; 43:1852-62.

11. Dalibor P, Shahaboddin S, Zˇarko Cˊ o, Vlastimir N, Nor Badrul A, Aznul QMS, et al. Adaptive Neuro-Fuzzy Estimation of Building Augmentation of Wind Turbine Power. Computer and Fluids. 2014; 97:188-94.

12. Wang B, Cotb LD, Adolphec L, Geoffroya S, Morchaind J. Estimation of Wind Energy Over Roof of two Perpendicular Buildings. Energy and Buildings. 2015; 88: 57–67.

13. Sharpe T, Proven G. Crossflex: Concept and Early Development Of A True Building Integrated Wind Turbine. Energy and Buildings. 2010; 42(12): 2365-75.

14. Peacock AD, Jenkins D, Ahadzi M, Berry A, Turan S. Micro Wind Turbines in the UK Domestic Sector. Energy and Building. 2008; 40:1324-33.

15. Mertens S, Delft T, Holland. Wind energy In Urban Areas: Concentration Effects for Wind Turbine Close to Buildings. Refocus. 2002:Pp. 22-4.

16. Ackermann T, Soder L. Wind Energy Technology and Current Status: A Review. Renewable and Sustainable Energy Reviews. 4, 315374, 2000. 2000;4:315-74.

17. Hyun B, Choi D, Han J, Jin J, Roo C. Performance analysis and Design of Vertical Axis Tidal Stream Turbine. Journal of Shipping and Ocean Engineering. 2012; 2:191-200.

18. Kentfield JAC. The Fundamentals of Wind-Driven Water Pumpers. London, United Kingdom: Taylor & Francis; 1996.

19. Johnson GL, Manhattan KS. Wind Energy Systems. 2001.

20. Hau E. Wind Turbines; Fundamentals, Technologies, Application, Economics. 2nd ed. Berlin, Germany: Springer; 2006.

21. Chong WT, Pan KC, Poh SC, Fazlizan A, Oon CS, Badarudin A, et al. Performance investigation of A Power Augmented Vertical Axis Wind Turbine for Urban High-Rise Application. Renew Energy. 2013; 51:388-97.

22. Beller C. Energy Output Estimation for a Small Wind Turbine Positioned on a Rooftop in the Urban Environment with and without a Duct. Riso-R-Report. 2011.

23. Valsamidis M. Wind Turbine Cross Wind Machine. US Patent No. 1995;US 5,380149.

24. Mertens S. The energy Yield Of Roof Mounted Wind Turbines. Wind Engineering. 2003; 27(6):507-17.

25. Mertens S. Wind Energy in the Built Environment: Concentrator Effects of Building [Thesis]. United Kingdom: Technische Universiteit Delft; 2006.

26. Sharpe T, Proven G. Crossflex: Concept and Early Development of A True Building Integrated Wind Turbine. Energy and Buildings. 2010; 42(12): 2365-75.

27. Ledo L, Kosasih PB, Cooper P. Roof Mounting Site Analysis for Micro-Wind Turbines. Renewable Energy. 2011; 36(5):1379-91.

28. Abohela I, Hamza N, Dudek S. Roof Mounted Wind Turbines: A Methodology for Assessing Potential Roof Mounting Locations. In: PLEA2013 - 29th Conference, Sustainable Architecture for a Renewable Future, 10-12 September 2013, Munich, Germany; 2013 .

29. Balduzzi F, Alessandro B, Ennio Antonio C, Lorenzo F., Magnani S. Feasibility Analysis of a Darrieus Vertical-Axis Wind Turbine Installation In the Rooftop of a Building. Applied Energy. 2012; 97: 921-9.

30. Strusnik D, Avsec J. Artificial Neural Networking Model of Energy and Exergy Districtheating Mony Flows. Energy and Buildings. 2015; 86:366–75.

31. Kecebas A, Yabanova I. Thermal Monitoring And Optimization of Geothermal District Heating Systems Using Artificial Neural Network: A Case Study. Energy and Buildings. 2012; 50:339–46.

32. Kecebas A, AliAlkan M, Yabanova I, Yumurtacı M. Energetic and Economic Evaluations of Geothermal District Heating Systems by Using ANN. Energy Policy. 2013; 56:558–67.

33. Kecebas A, Yabanova I, Yumurtacı M. Artificial neural Network Modeling of Geothermal District Heating System Thought Exergy Analysis. Energy Conversion and Management. 2012; 64:206–12.

34. Yabanova I, Keçebas A. Development of ANN Model For Geothermal District Heating System And A Novel PID-Based Control Strategy. Applied Thermal Engineering. 2013; 51:908-16.

35. Wei B, Wang S-L, Li L. Fuzzy comprehensive Evaluation of District Heating Systems. Energy Policy. 2010; 38: 5947–55.

36. Petkovic D, Shamshirband S, ojbašicˊ ZaC, Vlastimir N., Nor Badrul A, Aznul Qalid Md S, et al. Adaptive Neuro-Fuzzy Estimation of building Augmentation of Wind Turbine Power. Computer & Fluids. 2014; 97:188-94.

37. Chong WT, Gwani M, shamshirband S, Muzammil WK, Tan CJ, Fazlizan A, et al. Application of adaptive Neuro-Fuzzy Methodology for Perfomance Investigation of a Power-Augmented Vertical Axis Wind Turbine. Energy. 2016; 302:630-6.

38. Shamshirband S, Dalibor P, Nor Badrul A, Abdullah G. Adaptiveneuro-fuzzy Generalization of Wind Turbine Wake Added Turbulence Models. Renewable & Sustainable Energy Reviews. 2014; 36:270-6.

39. Vlastimir N, Petkovic D, Shamshirband S, Zarko C. Adaptive neuro-fuzzy Estimation of Diffuser Effects on Wind Turbine Performance. Energy. 2015; 89:324-33.

40. Mabel Carolin M, E. F. Analysis of Wind Power Generation and Prediction Using ANN: A Case Study. Renew Energy. 2008; 33:986-92.
41. Ragheb M. Optimal Rotor Wind Speed Ratio. 2014.
42. Kirke BK. Evaluation of Self-Starting Vertical Axis Wind Turbines for Stand-Alone Applications: Griffith Univerisity Gold Coast Campus; 1998.
43. Islam M, David SK, Ting AF. Aerodynamic Models for Darrieus-type straight-bladed Vertical Axis Wind Turbines. Renewable & Sustainable Energy Reviews. 2008; 12:1080-109.
44. Shamshirband S, Petkovic´ D, Saboohi H, Anuar NB, Inayat I, Akib S, et al. Wind Turbine Power Coefficient Estimation by Soft Computing Methodologies: Comparative Study. Energy Conversion & Management. 2014; 81:520-6.
45. Jang JSR. ANFIS: Adaptive-Network-based Fuzzy Inference Systems. IEEE Trans on Systems, Man and Cybernetics. 1993; 23(3): 665-85.
46. Ekici B, Aksoy U. Prediction of building Energy Needs In Early Stage of Design by Using ANFIS. Expert Systems with Applications. 2011; 38-5352.
47. Khajeh A, Modarress H, Rezaee B. Application of adaptive Neuro-Fuzzy Inference System for Solubility Prediction of Carbon Dioxide in Polymers. Expert Systems with Application. 2009; 36:5728.
48. Inal M. Determination of dielectric Properties of insulator Materials by Means of ANFIS: A Comparative Study. Expert Systems with Applications. 2008;195:34.

49. Petković D, Issa M, Pavlović ND, Pavlović NT, Zentner L. Adaptive Neuro-Fuzzy Estimation of Conductive Silicone Rubber Mechanical Properties. Expert Systems with Applications. 2012; 39: 9477-82.
50. Petković D ĆŽ. Adaptive neuro-Fuzzy Estimation of Automatic Nervous System Parameters Effect On Heart Rate Variability. Neural Computing & Application. 2012; 21(8):2065-70.
51. Petković D, Issa M, Pavlović ND, Zentner L, Ćojbašić Ž. Adaptive Neuro Fuzzy Controller for adaptive Compliant Robotic Gripper. Expert Systems with Applications. 2012; 39(18):13295-304.
52. Cam E, Yildiz O. Prediction of Wind Speed and Power in the Central Anatolian Region of Turkey by Adaptive Neuro-Fuzzy Inference Systems (ANFIS). Turkish J Eng Env Sci. 2006; 30:35-41.
53. Wahidabanu RSD, Shakilabanu A, Manoj D. Identification and Control of Nonlinear Systems using Soft Computing Techniques. International Journal of Modeling and Optimization. 2011; 1(1):24-8.
54. Grigorie TL, Botez RM. Adaptive Neuro-Fuzzy Inference System-Based Controllers For Smart Material Actuator Modelling. Journal of Aerospace Engineering. 2009; 223(6):655-68.
55. Akcayol MA. Application of Adaptive Neuro-Fuzzy Controller For SRM. Advances in Engineering Software. 2004; 35(3-4):129-37.